Supplementary Figures

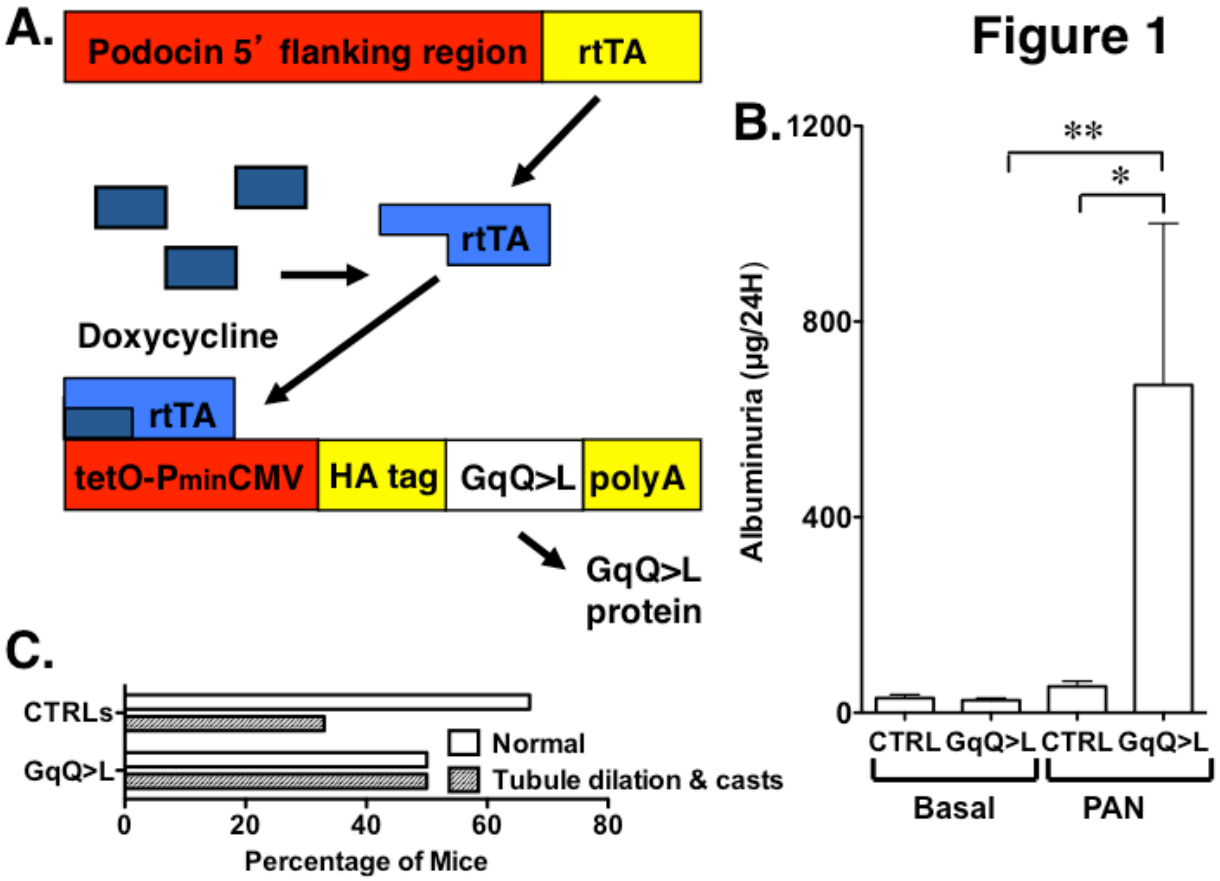

Figure 1. Effect of GqQ>L induction on PAN nephrosis. (A) Induction of GqQ>L requires 2 transgenic (TG) animals (1). The first TG animal expresses the reverse tetracycline transactivator (rtTA) under the control of the human podocin promoter (2). The second TG mouse expresses the HA (hemagglutinin) tagged GqQ>L construct under the control of tet operator sequence (tetO) and a minimal CMV promoter (PminCMV) (3). By breeding the two TG mice, animals were obtained that express both transgenes. In these "double" TG mice, treatment with doxycycline (DOX) induces transgene expression. (B) PAN induced a significant increase in albuminuria in mice expressing GqQ>L compared to both basal levels and PAN treated CTRLs. (C) Tubule dilation and casts tended to be more severe in GqQ>L mice compared to controls but this difference did not reach statistical significance. For the albuminuria and the histologic studies, we used 17 CTRLs and 14 GqQ>L mice. * $P<0.05$ or ** $P<0.01$ vs. the indicated groups using a Fisher's exact test for histologic data and an ANOVA followed by a Bonferroni post-hoc analysis for the albuminuria data.

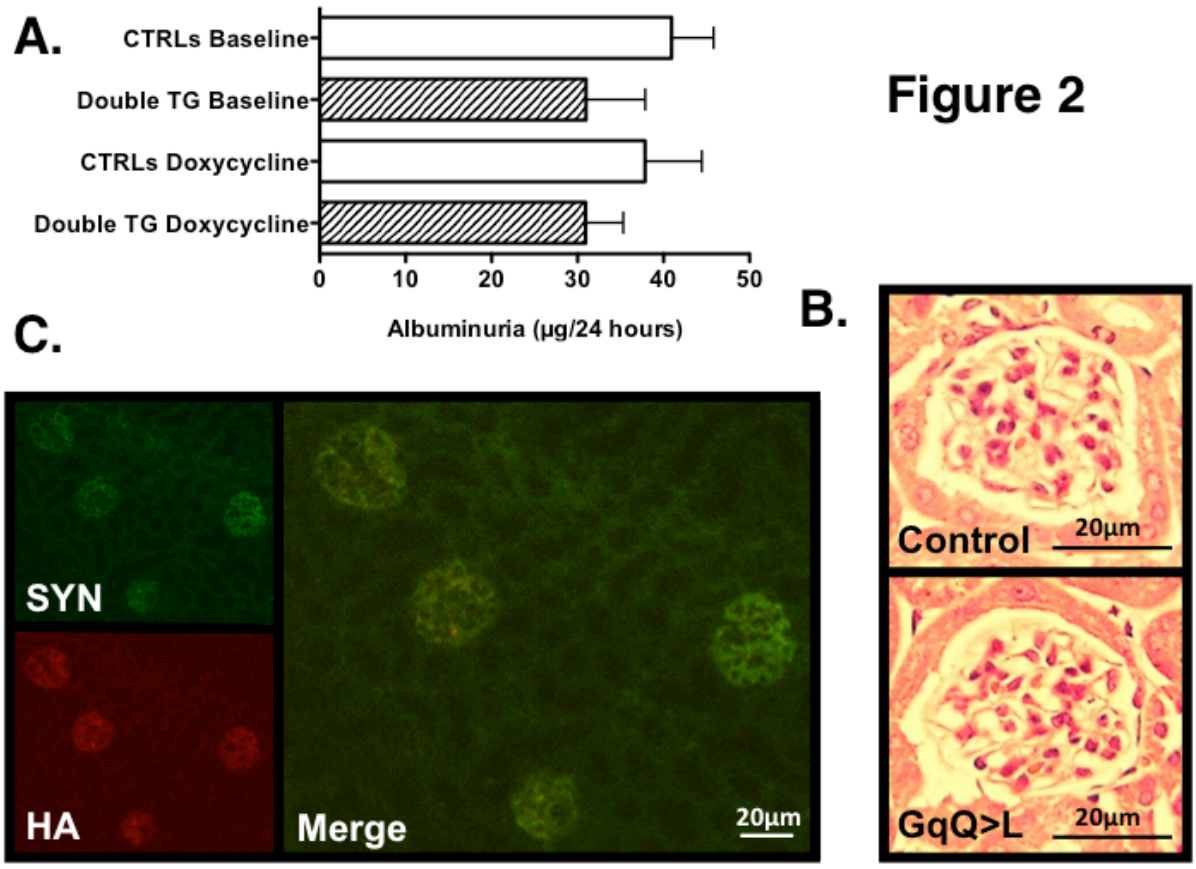

Figure 2

Figure 2. Effect of GqQ>L induction on albuminuria and glomerular histology. (A) Treatment of "double" TG GqQ>L mice with DOX alone did not induce albuminuria. (B) Glomerular histology was normal in "double" TG GqQ>L mice. Scale bars are 20 µm. (C) Tissue sections were stained for the podocyte marker synaptopodin (SYN) (fluorescein) and the HA tagged GqQ>L construct (CY3) as described in the Methods Section. Merging of the images suggested that the HA-tagged GqQ>L construct localized with the podocyte marker SYN. Scale bars are 20 µm. For the albuminuria and the light microscopic studies, 7-8 mice were studied per group. For the immunohistochemistry experiments, we studied 4 "double" TG GqQ>L mice and 3 CTRLs.

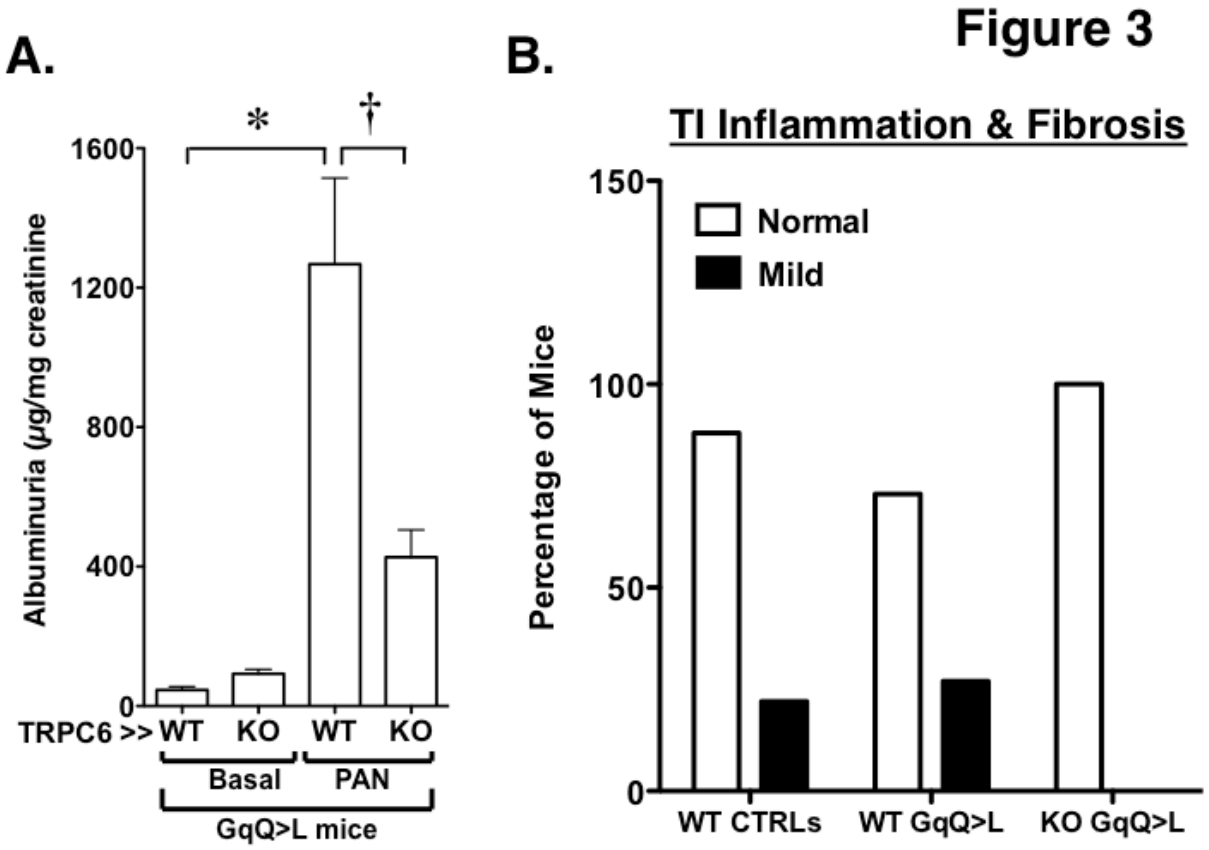

Figure 3. Effect of TRPC6 KO on PAN nephrosis in GqQ>L mice. (A) PAN caused a significant increase in albuminuria in WT mice expressing GqQ>L compared to basal levels. Albuminuria induced by PAN in GqQ>L mice lacking TRPC6 was significantly less compared to WT GqQ>L mice. (B) Tubulointerstitial (TI) inflammation and fibrosis tended to be more severe in WT GqQ>L mice compared to GqQ>L mice lacking TRPC6 but this change was not statistically significant. The albuminuria studies used 20 WT GqQ>L mice and 26 GqQ>L KO mice. The histology experiments used 8 WT CTRLs, 22 WT GqQ>L mice and 16 GqQ>L KO mice. †$P<0.05$ or *$P<0.005$ vs. the indicated groups using a Fisher's exact test for histologic data and an ANOVA followed by a Bonferroni post-hoc analysis for the albuminuria data.

Figure 4

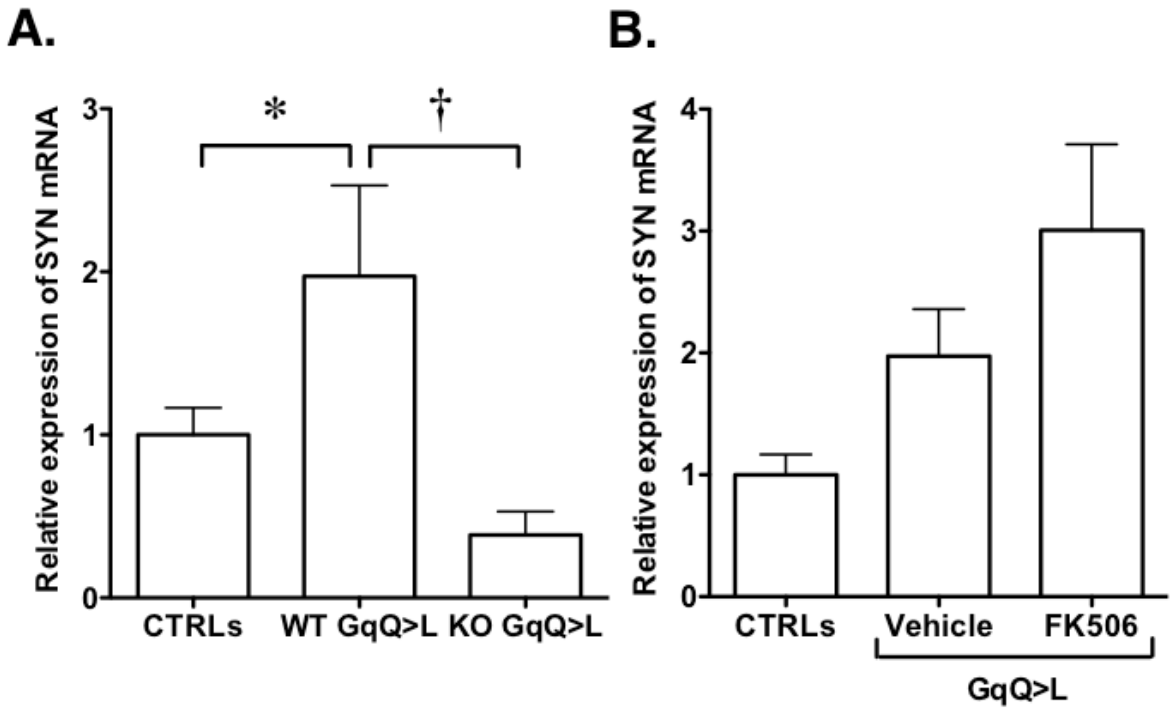

Figure 4. Effect of TRPC6 KO and FK506 on synaptopodin (SYN) mRNA levels in PAN nephrosis. (A) Expression of SYN mRNA was evaluated by quantitative real-time RT-PCR in CTRLs, WT GqQ>L mice and GqQ>L mice lacking TRPC6 (KO GqQ>L mice). SYN mRNA levels were significantly increased in WT GqQ>L mice compared to CTRLs. In KO GqQ>L mice, SYN RNA levels were significantly decreased compared to WT GqQ>L mice. (B) Expression of SYN mRNA levels tended to be increased in GqQ>L mice treated with either vehicle or FK506 compared to CTRLs, but these increases were not statistically significant. In panel A, we used mRNA samples from 12 WT CTRLs, 17 WT GqQ>L mice and 10 GqQ>L KO mice. In panel B, we used mRNA samples from 10 WT CTRLs, 16 vehicle treated GqQ>L mice and 6 FK506 treated GqQ>L mice. *$P<0.05$ or †$P<0.05$ vs. the indicated groups using an ANOVA followed by a Bonferroni post-hoc analysis.

Figure 5

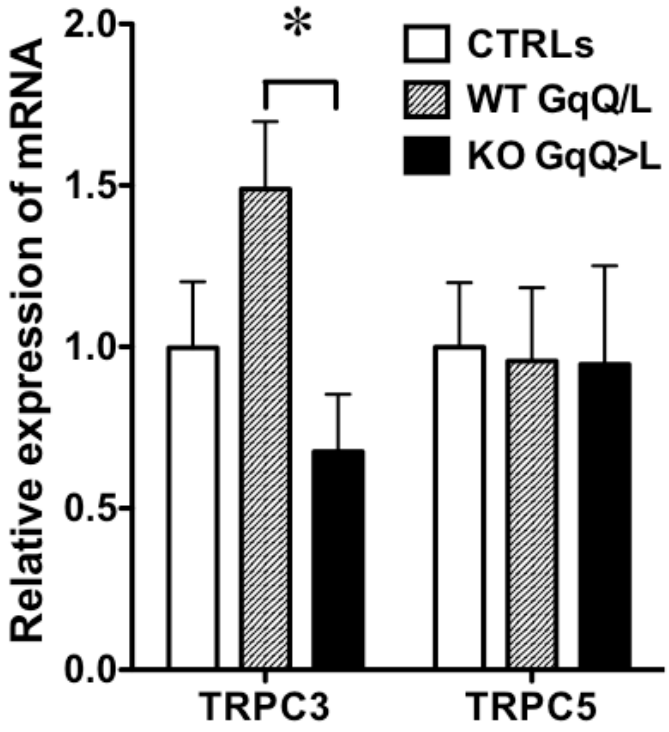

Figure 5. Effect of TRPC6 KO on mRNA levels of TRPC family members in PAN nephrosis. Expression of TRPC3 and TRPC5 mRNA was evaluated by quantitative real-time RT-PCR in PAN treated WT CTRLs, WT GqQ>L mice and GqQ>L mice lacking TRPC6 (KO GqQ>L mice). Relative expression of TRPC3 mRNA tended to be increased in WT GqQ>L mice compared to CTRLs but this difference was not statistically significant. In contrast, TRPC3 mRNA levels were significantly decreased in KO GqQ>L mice compared to WT GqQ>L mice. TRPC5 mRNA levels were similar in all groups. For Q-RT-PCR, we used mRNA samples from 12 WT CTRLs, 17 WT GqQ>L mice and 10 GqQ>L KO mice. *$P<0.05$ vs. the indicated groups using an ANOVA followed by a Bonferroni post-hoc analysis.

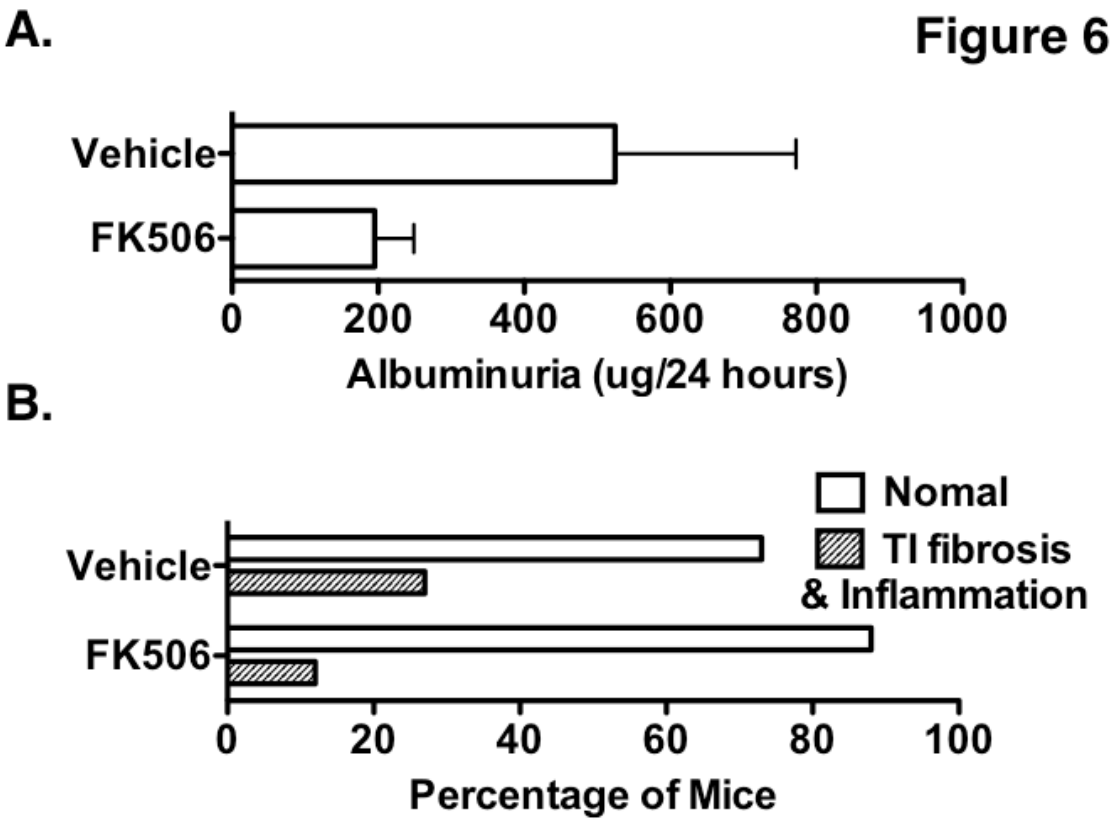

Figure 6. Effect of FK506 on PAN nephrosis in GqQ>L mice. (A) Treatment of GqQ>L mice with FK506 reduced albuminuria induced by PAN. (B) TI inflammation and fibrosis tended to be more severe in GqQ>L mice treated with vehicle compared to GqQ>L mice treated with FK506. For the albuminuria studies, we used 16 vehicle treated mice and 21 mice treated with FK506. For the histology studies, we used 16 vehicle treated mice and 8 mice treated with FK506. None of these differences were statistically significant using a Fisher's exact test for histologic data and a 2-tailed t-test for the albuminuria data.

Figure 7

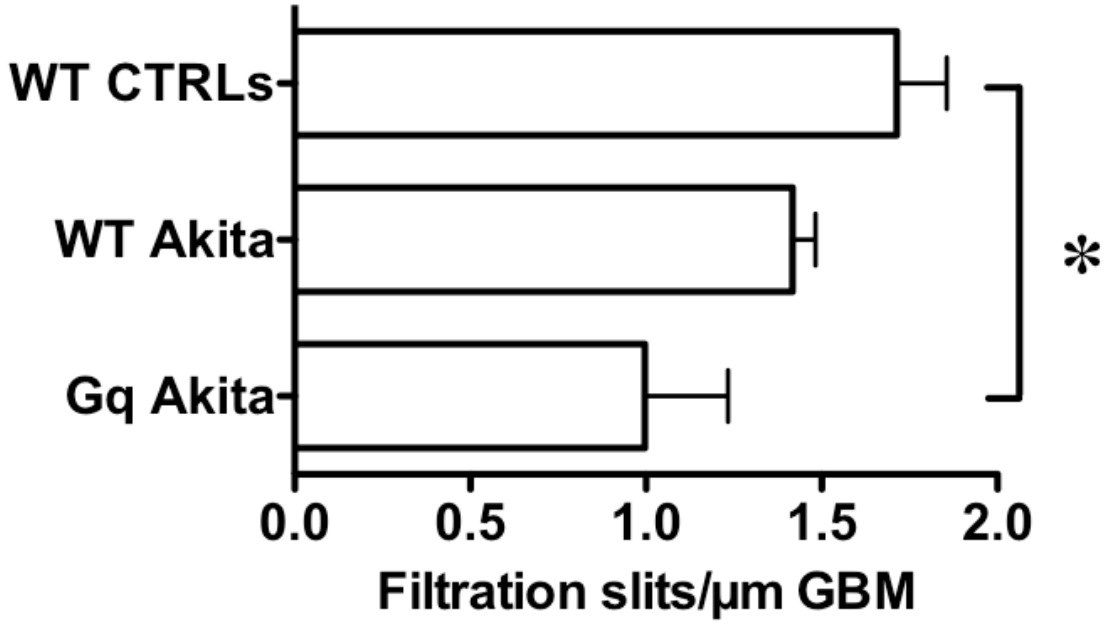

Figure 7. Effect of GqQ>L induction on foot process (FP) effacement. To quantitate FP effacement, we counted the number of filtration slits per micrometer (μm) glomerular basement membrane (GBM). FP flattening was more severe in the Akita mice expressing GqQ>L (Gq Akita mice). For the experiments, we studied 3 WT CTRLs, 3 WT Akita mice and 2 Gq Akita mice. *P<0.05 vs. the indicated groups using an ANOVA followed by a Bonferroni post-hoc analysis.

Figure 8

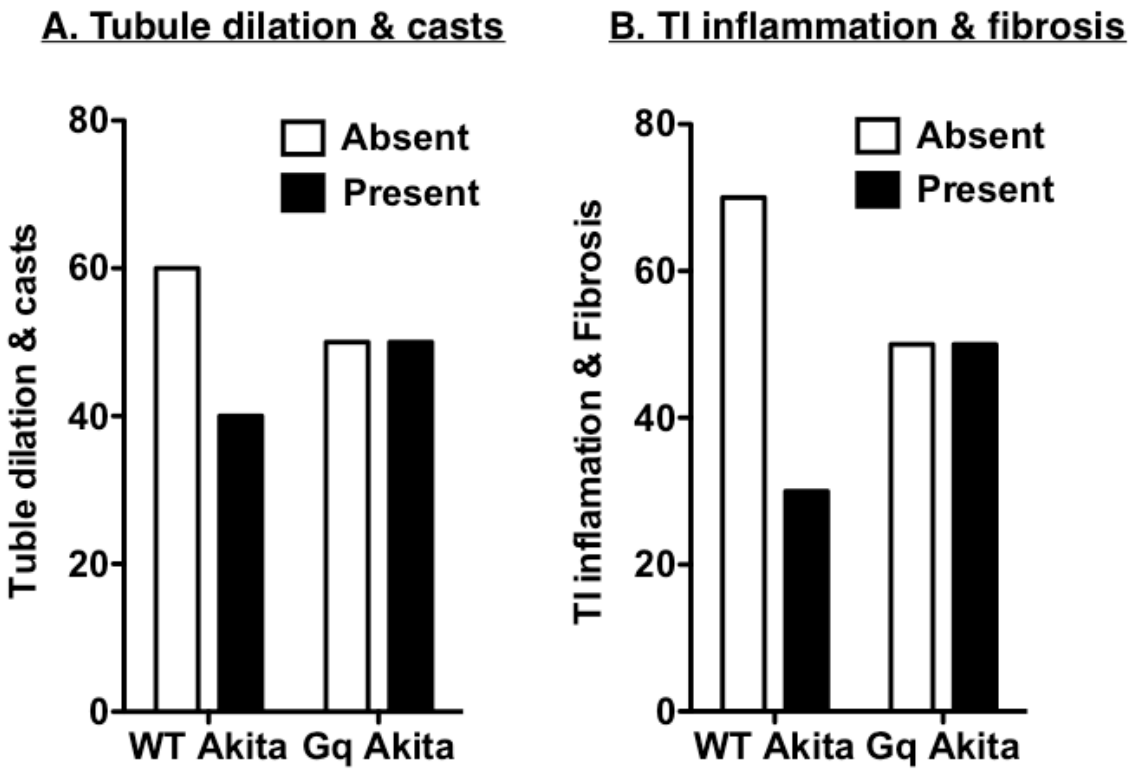

Figure 8. Effect of GqQ>L induction in Akita mice. (A & B) There were no significant differences in the severity of either tubule dilation and casts or tubulointerstitial (TI) inflammation and fibrosis between WT and Gq Akita mice. For the histologic studies, we used 18 WT Akita mice and 8 Gq Akita mice. Statistical analyses were performed using a Fisher's exact test.

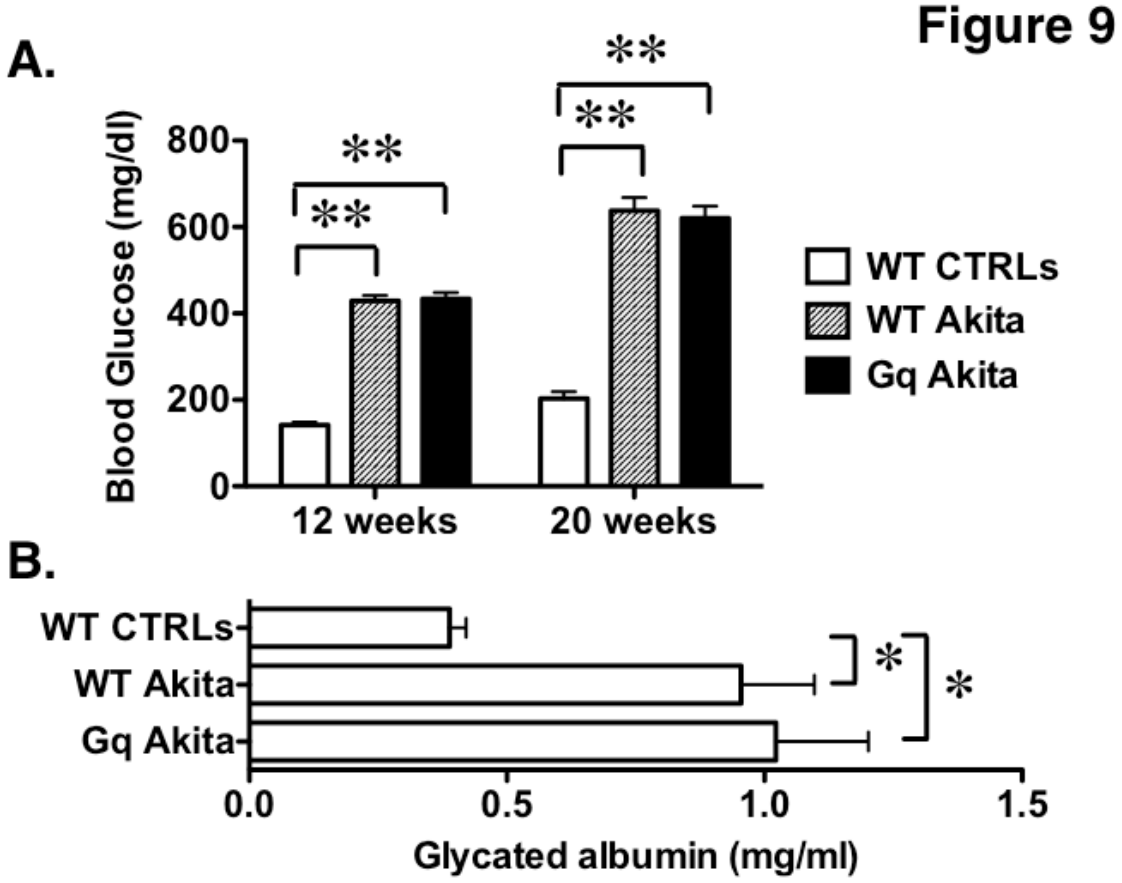

Figure 9. (A & B) Both blood glucose and glycated albumin levels were similarly elevated in Akita mice compared to non-diabetic, age and sex-matched WT CTRLs. For the studies, we used 14 WT CTRLs, 17 WT Akita mice and 8 Gq Akita mice. Glycated albumin was measured at 20 weeks of age. *P<0.05 or **P<0.005 vs. the indicated groups using ANOVA followed by a Bonferroni post-hoc analysis.

Figure 10

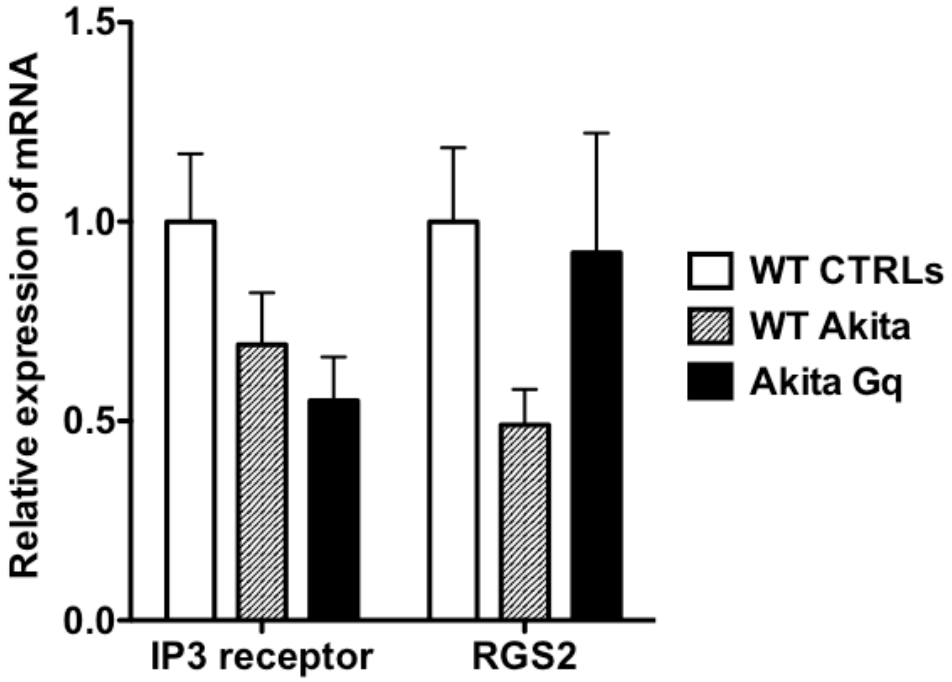

Figure 10. Effect of GqQ>L induction on expression of mRNA for the inositol trisphosphate (IP3) receptor and regulator of G protein signaling 2 (RGS2). IP3 receptor mRNA tended to be decreased in both groups of Akita mice. RGS2 mRNA tended to be increased in both WT CTRLs and Gq Akita mice compared to WT Akita mice. To assess mRNA expression we used glomerular samples from 13 CTRLs, 16 WT Akita mice and 7 Gq Akita mice. Statistical analyses were performed using an ANOVA followed by a Bonferroni post-hoc analysis.

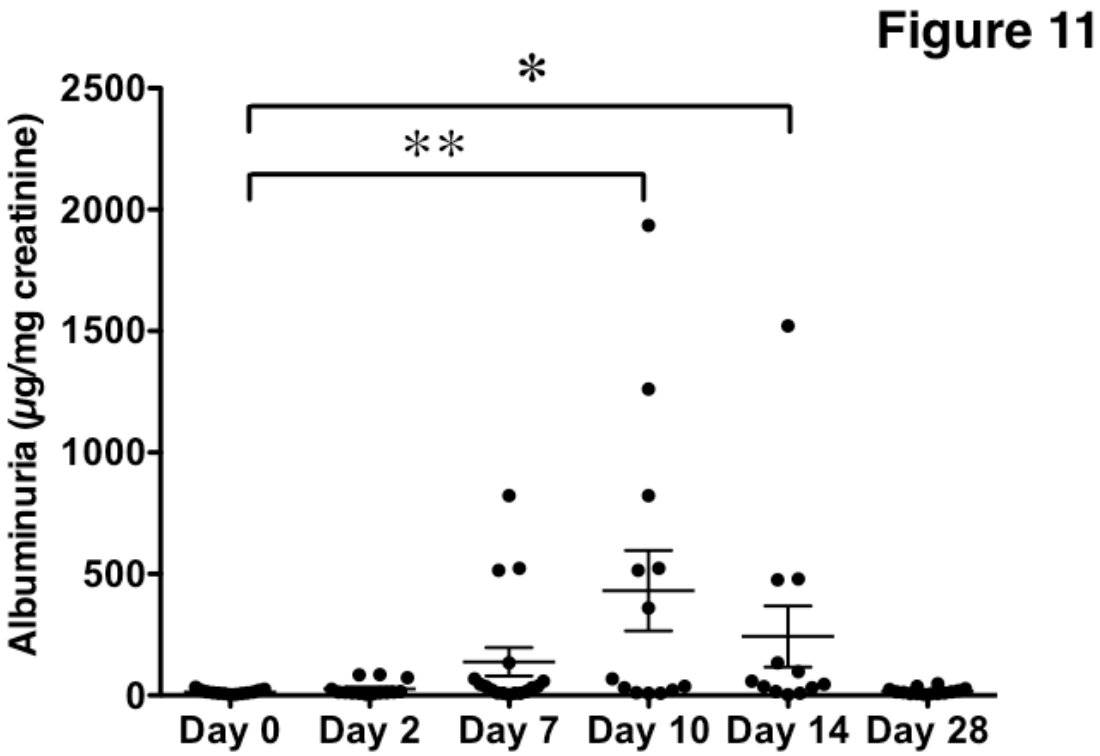

Figure 11. Time course of albuminuria in PAN nephrosis in WT CTRL mice. Pilot studies were performed to determine the time course of PAN nephrosis in WT CTRLs. Albuminuria was significantly increased at both 10 and 14 days after treatment with PAN and then returned to baseline by day 28. For the experiments, 13-16 mice were studied at each time point. *P<0.05 or **P<0.01 vs. the indicated groups using an ANOVA followed by a Bonferroni post-hoc analysis.

Supplementary Methods

Reverse transcription (RT) followed by a quantitative polymerase chain reaction (Q-RT-PCR): The following sequences were used for mouse TRPC6, COX2, RCAN1, RGS2 and IP3 receptor: TRPC6 forward, 5'- TGC TTG ACT TTG GAA TGC TG -3'; reverse, 5'- GTT GTC CCC CAG TGT GAC TT -3'; COX2 forward, 5'- TGC AGA ATT GAA AGC CCT CT -3'; reverse, 5'- CCC CAA AGA TAG CAT CTG GA -3'; RCAN1 forward, 5'- CTC CTC CCG TTG GCT GGA AA -3'; reverse, 5'- CTG GGA GTG GTG TCT GTC GC; IP3 receptor forward, 5' – TAC AAG GGA CCA GGA TTT GC; reverse 5'- GTC AGA CAT GTC CGT GTT GG - 3'; RGS2 forward, 5'- TTT TCT CCC GCT TCT CCT CG - 3'; reverse, 5'- CAA AGT GCC ATG TTC CTG GC - 3'; Cyclophilin, 5' – GGCCGATGACGAGCCC – 3'; reverse, 5' – TGTCTTTGGAACTTTGTCTGCAA – 3'.

Glomerular Basement Membrane (GBM) Width: In the Akita studies, GBM width was measured using the orthogonal intercept technique (4) and Photoshop CS6 Extended after calibrating the measurement tool to convert pixels to a known distance in the digital images. For the actual measurements, the Photoshop software was used to place a grid over the digital images by choosing View>Show>Gridlines. At the intercept of each gridline, the minimal distance between the endothelial and epithelial cell membranes was measured (orthogonal intercept) avoiding the mesangial areas (5). An average of 72 ± 22 measurements were obtained per capillary loop and an average of 11.5 ± 1.2 capillary loops were examined per mouse. The harmonic mean of these measurements was then corrected for oblique sectioning using the correction factors described by Ramage et al (6). All images were evaluated without knowledge of either genotype or experimental group.

Quantitation of podocyte number, podocyte density and glomerular volume: To estimate podocyte density [Nv(P/Glom)] we used the method of Weibel and Gomez (7) based on the following considerations: 1. The method does not require complete glomeruli for average podocyte number estimates (8), 2. The method of Weibel and Gomez correlates well with more rigorous methodologies (9), and 3. This methodology is the method of choice when a limited tissue sample is available (8) as was the case in the current study (most of the kidney tissue in the present study was used for glomerular isolation and the remaining sample was divided among light microscopy, TEM and fluorescent microscopy). For these experiments, podocyte nuclei were stained with the WT1 antibody (fluorescein), the glomerular tuft was stained with the synaptopodin antibody (rhodamine) and nuclei were stained with DAPI as described above. An average of 22 ± 0.5 glomeruli (range 12-32) were evaluated in the tissues specimens. Digital images of tissue sections were taken using confocal microscopy to insure that the section thickness was less than the mean caliper diameter of the podocyte nuclei (8). To calculate podocyte density using the method of Weibel and Gomez we used the equation described by White and Bilous (9):

$$Nv = K/\beta\sqrt{(N_A{}^3/Vv)}$$

where N_A is the profile density (9) or the number podocyte nuclei per glomerular surface area (10), Vv is the volume density (9) or the ratio of podocyte nuclear volume to the glomerular volume (10), K is the size distribution coefficient value of 1.01 and β is the shape constant of 1.55. The number of podocyte nuclei per glomerulus was obtained by counting the number of podocyte nuclei that both co-localized with DAPI as well as WT1 and were associated with synaptopodin staining. Photoshop CS6 Extended was used to determine the glomerular area

(A_G) after a calibrating the measurement tool to convert pixels to a known surface area. The glomerular area in the digital images was then outlined using the "lasso" tool and the number of pixels in the glomerular area determined using the histogram function, which can then be converted to the glomerular area. N_A is then obtained by dividing the number of podocyte nuclei by the glomerular area. The measurement of Vv takes advantage of the theorem developed by Delesse (10), which states that the areal density (A_A) of a feature of interest in the reference compartment in 2 dimensional space is directly proportional to Vv. Thus, A_A is equal to Vv (10). For the actual measurements, the Photoshop software was used to place a grid over the digital images by choosing View>Show> Gridlines. The number of points overlying podocyte nuclei divided by the number of points overlying the glomerular area is directly proportional to A_A, which is equal to Vv (10).

The mean glomerular volume (VGlom) was obtained from the arithmetic mean of the glomerular surface area (AGlom) using the method of Weibel and the equation described by Gundersen and coworkers (11):

$$VGlom = K/\beta \times (A_G)^{3/2}$$

where A_G was obtained as described above, K = 1.10 is the distribution coefficient and β = 1.38 is the shape coefficient, which pertains to spheres. An estimate of the total number of podocytes per glomerulus [N(P/Glom)] was obtained by multiplying Nv(P/Glom) by the glomerular volume (VGlom) (8). All measurements were made without knowledge of either genotype or experimental group.

References

1. Gingrich, JR, and Roder, J. Inducible gene expression in the nervous system of transgenic mice. *Annu Rev Neurosci*. 1998; 21:377-405.
2. Shigehara, T, Zaragoza, C, Kitiyakara, C, Takahashi, H, Lu, H, Moeller, M, Holzman, LB, and Kopp, JB. Inducible podocyte-specific gene expression in transgenic mice. *J Am Soc Nephrol*. 2003; 14:1998-2003.
3. Wang, L, Flannery, PJ, Rosenberg, PB, Fields, TA, and Spurney, RF. Gq-dependent signaling upregulates COX2 in glomerular podocytes. *J Am Soc Nephrol*. 2008; 19:2108-2118.
4. Jensen, EB, Gundersen, HJ, and Osterby, R. Determination of membrane thickness distribution from orthogonal intercepts. *J Microsc*. 1979; 115:19-33.
5. Das, AK, Pickett, TM, and Tungekar, MF. Glomerular basement membrane thickness - a comparison of two methods of measurement in patients with unexplained haematuria. *Nephrol Dial Transplant*. 1996; 11:1256-1260.
6. Ramage, IJ, Howatson, AG, McColl, JH, Maxwell, H, Murphy, AV, and Beattie, TJ. Glomerular basement membrane thickness in children: a stereologic assessment. *Kidney Int*. 2002; 62:895-900.
7. Weibel, ER, and Gomez, DM. A principle for counting tissue structures on random sections. *J Appl Physiol*. 1962; 17:343-348.
8. Lemley, KV, Bertram, JF, Nicholas, SB, and White, K. Estimation of glomerular podocyte number: a selection of valid methods. *J Am Soc Nephrol*. 2013; 24:1193-1202.
9. White, KE, and Bilous, RW. Estimation of podocyte number: a comparison of methods. *Kidney Int*. 2004; 66:663-667.
10. Bertram, JF. Analyzing renal glomeruli with the new stereology. *Int Rev Cytol*. 1995; 161:111-172.
11. Hirose, K, Osterby, R, Nozawa, M, and Gundersen, HJ. Development of glomerular lesions in experimental long-term diabetes in the rat. *Kidney Int*. 1982; 21:689-695.